

See discussions, stats, and author profiles for this publication at: <https://www.researchgate.net/publication/8567181>

Biofunctionalized Polymer Surfaces Exhibiting Minimal Interaction towards Immobilized Proteins

ARTICLE *in* CHEMPHYSCHEM · APRIL 2004

Impact Factor: 3.42 · DOI: 10.1002/cphc.200400024 · Source: PubMed

CITATIONS

68

READS

55

7 AUTHORS, INCLUDING:



Jürgen Groll

University of Wuerzburg

121 PUBLICATIONS 2,335 CITATIONS

SEE PROFILE



Thomas Ameringer

Swinburne University of Technology

12 PUBLICATIONS 538 CITATIONS

SEE PROFILE



Carlheinz Röcker

Universität Ulm

49 PUBLICATIONS 2,399 CITATIONS

SEE PROFILE



Martin Möller

RWTH Aachen University

638 PUBLICATIONS 14,296 CITATIONS

SEE PROFILE

Biofunctionalized Polymer Surfaces Exhibiting Minimal Interaction towards Immobilized Proteins

Elza V. Amirgoulova,^[a] Jürgen Groll,^[b] Colin D. Heyes,^[a] Thomas Ameringer,^[b] Carlheinz Röcker,^[a] Martin Möller,^[c] and G. Ulrich Nienhaus^{*[a, d]}

Biomolecules exhibit remarkable sensitivity, selectivity and efficiency in their response to specific stimuli, which makes them extremely attractive targets for sensor applications.^[1] Biosensor designs are often based on hybrid (biotic–abiotic) nanoscale interface technologies, in which biomolecules are immobilized on solid substrates.^[2,3] The delicate structure of proteins requires coating of these surfaces with carefully designed films that interact only weakly with the protein, except through a strong tether for protein attachment, and thus preserve the functionally competent, properly folded conformation. The surface must not only resist interaction with the hydrophilic surface of the native protein structure, rather, for stability over long periods of times and/or under destabilizing conditions (extreme temperatures, cosolvents), the surface must also be inert towards hydrophobic protein moieties that become transiently or permanently exposed upon unfolding. Here we present a versatile surface preparation that matches exactly these requirements. It was specifically developed for single-molecule studies of protein folding, the intriguing process by which the linear polypeptide chain assumes its specific, functionally competent three-dimensional architecture.^[4–6]

Protein folding is an intrinsically heterogeneous process because a huge number of folding pathways on the free energy surface connect the myriad of unfolded conformations with the much smaller set of conformations belonging to the native state.^[7] Förster resonance energy transfer (FRET) between a donor and acceptor fluorophore has been used extensively in equilibrium and time-resolved investigations of protein folding on large protein ensembles.^[8–10] With the advent of single-molecule fluorescence spectroscopy, a technique has become available that enables us to examine protein folding pathways of individual protein molecules in real time, and to detect intermediate states and trajectories leading to misfolded structures, which have been implicated in diseases such as the

spongiform encephalopathies (BSE, CJD, Alzheimer's disease).^[11] The strong distance dependence of FRET can be exploited to observe the reconfiguration of a single polypeptide chain in real time.^[12] To this end, a donor–acceptor pair of fluorescent dye molecules is attached to specific locations along the polypeptide chain so that the two dyes are in close proximity in the folded structure and further apart in the unfolded chain. Such experiments, performed on proteins diffusing freely in solution,^[13,14] have already yielded insightful results. Free diffusion, however, limits the observation time to the transit time of the protein through the sensitive volume of the microscope, which is typically less than 1 ms. Longer observation time can be realized by fixing the molecules in space to within a volume smaller than the extent of the point-spread function of the microscope. Immobilization of proteins inside surface-bound lipid vesicles is an elegant approach,^[15] but this does not allow easy solvent exchange. More versatile is the direct tethering of the protein to the surface. This strategy has been pursued to observe conformational dynamics of a small peptide on an amino-silylated glass surface.^[16] In close proximity to a nanostructured surface, a biomolecule experiences an environment that is distinctly different from that in solution. Surface-protein interactions can easily be in the range of the overall stabilization energy of the native fold and thus can profoundly change the energy landscape of the protein. Therefore, experiments with surface-immobilized proteins reveal properties of the protein-surface assembly and not of the protein alone—unless a suitable surface treatment ensures minimal mutual interactions.

We have developed nanostructured surfaces with excellent properties for protein functionalization even under destabilizing conditions. These polymer coatings on glass or quartz substrates are based on poly(ethylene glycol) (PEG), hydrophilic and uncharged polymers known to resist unspecific protein adsorption.^[17,18] While both star-shaped and linear PEGs have this advantageous property,^[19] linear, non-crosslinked PEG chains have been observed to stabilize the unfolded state of immobilized proteins by intermingling with the polypeptide chains.^[20] Therefore, we have employed a six-arm star-shaped PEG (molecular mass ≈ 12 kDa) in this work. Numerous ways have been devised to end-functionalize PEGs for their attachment to surfaces^[21] and biomolecules.^[22,23] Here we have used reactive isocyanate groups at the ends of the star-polymer arms for binding to amine groups on the glass surface and crosslinking with each other. Moreover, a small fraction of isocyanate groups was biotinylated to enable protein functionalization via the biotin–streptavidin linkage.^[24,25]

Our star-polymer surfaces are produced by spin-casting an aqueous solution of a six-arm star-shaped pre-polymer (molecular mass ≈ 12 kDa) on an amino-silylated glass or quartz substrate. Once the film is formed, all isocyanate groups have been converted into urea cross-linking bridges or free amines. Film thicknesses were determined by ellipsometry to be 5 ± 0.5 nm. Excellent surface smoothness was revealed by AFM, and single-molecule fluorescence experiments showed an extremely low level of nonspecific adsorption for a variety of proteins (streptavidin, avidin and RNase H). Surfaces could be pre-

[a] E. V. Amirgoulova, C. D. Heyes, C. Röcker, Prof. G. U. Nienhaus
Department of Biophysics, University of Ulm
Albert Einstein Allee 11, 89081 Ulm (Germany)
Fax: (+49) 731-502-3059
E-mail: uli@uiuc.edu

[b] J. Groll, T. Ameringer
Department of Macromolecular Chemistry and Organic Chemistry III
University of Ulm, Albert Einstein Allee 11, 89081 Ulm (Germany)

[c] M. Möller
Deutsches Wollforschungsinstitut an der RWTH Aachen und Institut für
Technische und Makromolekulare Chemie der RWTH Aachen
Veltmanplatz 8, 52062 Aachen (Germany)

[d] Prof. G. U. Nienhaus
Department of Physics, University of Illinois Urbana-Champaign
Urbana, Illinois, 61801 (USA)

pared and stored in sealed Petri-dishes for several months prior to use, which indicates long-term stability of the cross-linked star-polymer surfaces. The star-polymer surfaces are statistically decorated with biotin, to which streptavidin is bound. The vacant biotin binding sites on the streptavidin can then serve as anchors to enable specific molecular recognition of biotinylated proteins. Herein, we have immobilized RNase H on the star-polymer surface, a small enzyme that serves as a model system in protein folding. For FRET experiments, a pair of Alexa 546/647 dyes was attached via maleimide groups to cysteines introduced at positions 3 and 135 along the RNase H polypeptide chain. A schematic of the entire nanostructured assembly is given in Figure 1.

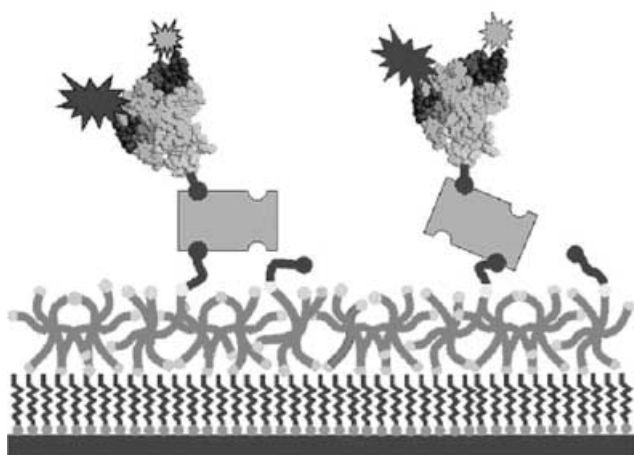


Figure 1. Schematic of our inert, biofunctionalized surfaces. Amino-silylated glass is coated with a layer of cross-linked six-arm star polymers, to which fluorescently labeled RNase H is coupled via a streptavidin-biotin linkage.

The immobilized RNase H shows a completely reversible transition between native and denatured conformations upon alternating between denaturing solvent (6 M guanidinium chloride, GdmCl) and buffer [20 mM Tris-HCl (tris(hydroxymethyl)aminomethane), 100 mM KCl, 10 mM MgCl₂, pH 7.4]. This is evident from the three confocal microscopy images in Figure 2 (top row), which were taken before adding denaturant, after adding denaturant, and after removal of denaturant by washing with buffer. These images are overlays of data acquired simultaneously in the donor (green) and acceptor (red) channels of our confocal fluorescence microscope upon excitation of the donor dye at 514 nm. Individual RNase H molecules immobilized on a star-polymer surface are shown as red,

green and yellow spots. The fractions of folded and unfolded molecules can be extracted from the images by calculating the FRET efficiency [Equation (1)],

$$E = \frac{I_A}{I_A + \gamma I_D} \quad (1)$$

for each molecule. Here, I_D and I_A are the photon counts in the donor and acceptor channels for each spot, and γ is a correction factor that accounts for the different fluorescence quantum yields and detection efficiencies for donor and acceptor emission. In the bottom row, Figure 2 presents histograms of the number of molecules with particular values of E . The lines in the histogram represent (normal and log-normal) model distributions with which the data were fitted to quantify the various components.^[13] Before denaturation and after renaturation, the histograms are identical within the experimental error. A predominant distribution of molecules at $E \approx 1$ (depicted in red in Figure 2a), represents folded proteins, which have small donor-acceptor distances (red spots in the image). Another peak at $E \approx 0$ is due to molecules lacking an acceptor dye (green spots). Under denaturing conditions, there are no red spots, and consequently, the histogram does not contain any molecules with $E \approx 1$. Rather, there is a large and broad distribution of molecules centred at $E \approx 0.3$ (depicted in yellow in Figure 2b). The low FRET efficiency implies a significantly increased donor-acceptor distance. This distribution thus represents unfolded proteins (yellow spots), as has been noticed earlier for diffusing protein molecules.^[13,14] Quantitatively, the FRET efficiency depends on the sixth power of the donor-acceptor distance R , [Equation (2)].

$$E = \frac{R_0^6}{R_0^6 + R^6} \quad (2)$$

Here, R_0 is the characteristic Förster distance of the donor-

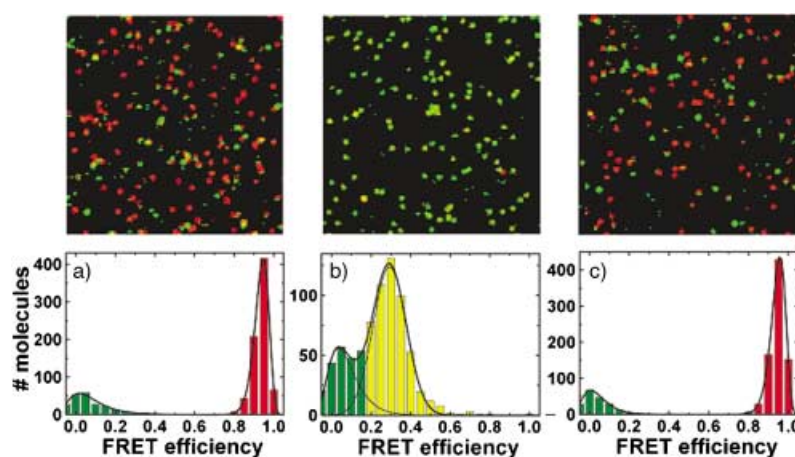


Figure 2. Alternating exposure of surface-immobilized RNase H molecules to a) buffer solution, b) 6 M guanidinium chloride as denaturant, and c) again buffer solution, showing complete reversibility of the denaturation transition. Top: Examples of two-colour (green/red) overlay confocal scan images (18 $\mu\text{m} \times 18 \mu\text{m}$) upon laser excitation of the green dye at 514 nm; bottom: histograms of molecules with particular values of FRET efficiencies E , showing distributions corresponding to folded RNase H molecules (red, $E \approx 1$), denatured molecules (yellow, $E \approx 0.3$), and molecules without red acceptor dye (green, $E \approx 0$).

acceptor dye pair used, which in our case is 71 Å in 6 M GdmCl. $E \approx 0.3$ thus corresponds to an average donor–acceptor separation of $R \approx 82$ Å, which is in excellent agreement with small-angle scattering data on a variety of proteins under denaturing conditions.^[26] Due to the heterogeneous nature of the protein coil, however, there is a broad distribution of FRET efficiencies around 0.3.

To demonstrate the resilience of the surface-immobilized biomolecules against permanent denaturation, we subjected samples to many consecutive cycles of denaturation–renaturation. In Figure 3a and b, we show confocal images of a small,

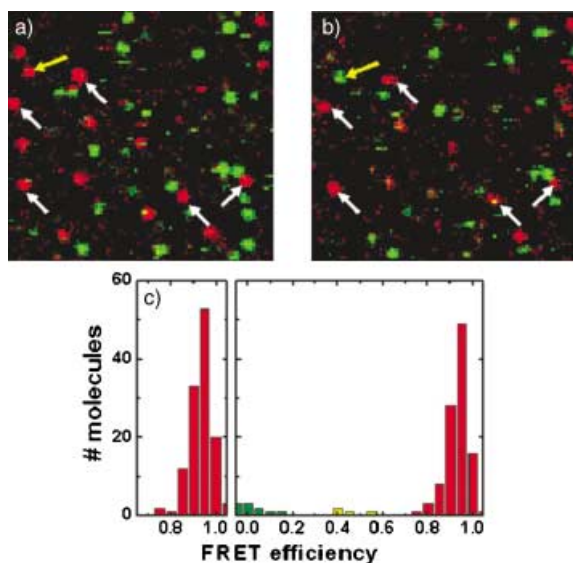


Figure 3. Confocal fluorescence microscopy scans of the same $10\ \mu\text{m} \times 10\ \mu\text{m}$ sized area a) before and b) after 50 consecutive cycles of denaturation–renaturation (3 h later). Five molecules are highlighted by white arrows to show that they can be tracked over long times. For some molecules, photobleaching of the red dye occurs; an example is marked by the yellow arrow. c) FRET histograms of 126 folded molecules before (left frame) and after (right frame) the 50 denaturation cycles, showing that four molecules became trapped in an unfolded conformation (yellow), and 10 had lost their acceptor dye $E \approx 0$ (green). The vast majority retained their folded configuration.

$10\ \mu\text{m} \times 10\ \mu\text{m}$ section of a sample, taken before and after 50 cycles of denaturation with 6 M GdmCl and subsequent renaturation with buffer. The corresponding FRET distributions are plotted in Figure 3c. From 116 molecules carrying a donor–acceptor pair, only four were observed in a low-FRET state ($0.4 < E < 0.6$) after the experiment, which is indicative of a nonnative conformation. The vast majority were able to refold completely after each cycle.

To examine surface interactions with the protein, we measured the equilibrium between folded and unfolded states as a function of denaturant concentration, [GdmCl]. The free energy difference, ΔG_{FU} , is related to the population ratio of unfolded (U) and folded (F) molecules by Equation (3).

$$\Delta G_{\text{FU}} = -RT \ln \frac{U}{F} \quad (3)$$

Here, R and T denote the gas constant and absolute temperature (in K), respectively. Near the titration midpoint, ΔG_{FU} depends approximately linearly on [GdmCl] as shown in Equation (4),

$$\Delta G_{\text{FU}} = \Delta G_0 - m[\text{GdmCl}] \quad (4)$$

where ΔG_0 is the extrapolation to zero denaturant concentration, and the slope (m value) quantifies the cooperativity of folding.^[27]

Figure 4a shows an overlay image of RNase H molecules near the titration midpoint, at [GdmCl] = 1.7 M. The corresponding histogram of the number of molecules as a function of E is

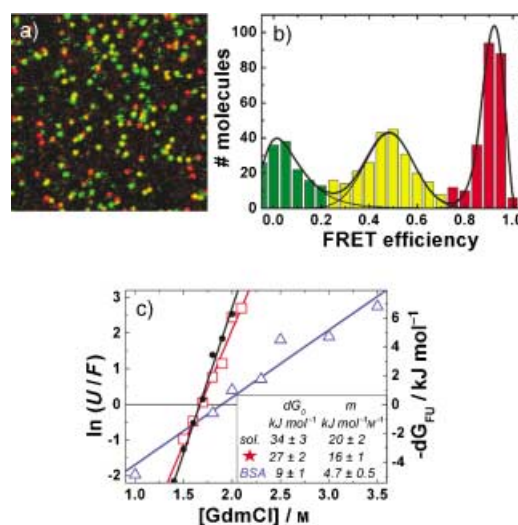


Figure 4. Titration of surface-immobilized and dissolved RNase H molecules with the denaturant GdmCl. a) Two-colour confocal scan image of RNase H immobilized on a star-polymer surface and fluorescently labeled with a FRET pair of dyes at [GdmCl] = 1.7 M, b) corresponding FRET efficiency histogram, and c) logarithm of population ratios and resulting free energy differences between folded and unfolded conformations, ΔG_{FU} , plotted as a function of GdmCl concentration, of RNase H in buffer solution (black), RNase H immobilized on star-polymer (red) and physisorbed BSA (blue) surfaces; c) inset gives the experimentally determined values of standard free energy, ΔG_0 , and cooperativity, m , for the protein in different environments.

presented in Figure 4b. These histograms were fitted with three (normal and log-normal) distributions^[13] (see the lines in Figure 4b). From the areas under the yellow and red distributions, the fractions of unfolded and folded molecules were determined, respectively, and ΔG_{FU} was calculated with Equation (3). In Figure 4c, ΔG_{FU} of RNase H on star-polymer surfaces (red symbols) is shown for seven different values of [GdmCl]. A linear fit (red line) yields the parameters ΔG_0 and m [Equation (3)], given in the inset. Also included (in blue) are data and fit from an experiment in which RNase H was linked via biotin-streptavidin to surface-adsorbed, biotinylated bovine serum albumin (BSA). This is a simple and widely used procedure to immobilize biomolecules for single-molecule studies.^[28,29] For comparison, we have also measured the [GdmCl] dependence of an RNase H molecule freely diffusing in solu-

tion (black). With the star-polymer-derived surfaces, a steep dependence on [GdmCl] is observed; essentially identical to the behaviour of the solution sample. This measurement clearly shows the weakly interacting nature of the star-polymer surface with the immobilized RNase H molecules. Therefore, this result offers convincing evidence that the free energy surfaces of the immobilized RNase H molecules on the star-polymer surfaces are the same as in solution. In contrast, for the BSA-coated surface the slope is much less, reflecting significantly larger interaction of the RNase H with this surface.

The single-molecule studies presented here have shown that our cross-linked, star-polymer-derived surfaces not only allow reversible unfolding and refolding, but also interact negligibly with the immobilized proteins. For this important reason, they are superb surfaces for the study of immobilized biomolecules, especially by using single-molecule techniques.

Acknowledgements

C.D.H. would like to thank the Alexander von Humboldt Foundation and the Human Frontiers Science Program (HFSP) for research fellowships. We also thank Uwe Theilen for help in the expression and purification of the RNase H. Financial support from the Deutsche Forschungsgemeinschaft (SFB569) is gratefully acknowledged.

Keywords: biosensors • polymers • protein folding • single-molecule studies • surface chemistry

- [1] A. P. F. Turner, *Science* **2000**, 290, 1315–1317.
- [2] J. F. Klemic, E. Stern, M. A. Reed, *Nature Biotech.* **2001**, 19, 924–925.
- [3] A. J. Haes, R. P. V. Duyne, *J. Am. Chem. Soc.* **2002**, 124, 10596–10604.
- [4] J. D. Bryngelson, J. N. Onuchic, N. D. Socci, P. G. Wolynes, *Prot. Struct. Funct. Gen.* **1995**, 21, 167–195.
- [5] C. M. Dobson, A. Sali, M. Karplus, *Angew. Chem.* **1998**, 110, 868–893; *Angew. Chem. Int. Edit.* **1998**, 37, 868–893.
- [6] H. S. Chan, K. A. Dill, *Phys. Today* **1993**, 46, 24–32.
- [7] P. G. Wolynes, J. N. Onuchic, D. Thirumalai, *Science* **1995**, 267, 1619–1620.
- [8] K. Teilum, K. Maki, B. B. Kragelund, F. M. Poulsen, H. Roder, *Proc. Natl. Acad. Sci. USA* **2002**, 99, 9807–9812.
- [9] J. G. Lyubovitsky, H. B. Gray, J. R. Winkler, *J. Am. Chem. Soc.* **2002**, 124, 5481–5485.
- [10] C. Nishimura, R. Riley, P. Eastman, A. L. Fink, *J. Mol. Biol.* **2000**, 299, 1133–1146.
- [11] C. M. Dobson, *Nature* **2002**, 418, 729–730.
- [12] S. Weiss, *Nat. Struct. Biol.* **2000**, 7, 724–729.
- [13] B. Schuler, E. A. Lipman, W. A. Eaton, *Nature* **2002**, 419, 743–747.
- [14] A. A. Deniz, T. A. Laurence, G. S. Beligere, M. Dahan, A. B. Martin, D. S. Chemla, P. E. Dawson, P. G. Schultz, S. Weiss, *Proc. Natl. Acad. Sci. USA*, **2000**, 97, 5179–5184.
- [15] E. Rhoades, E. Gussakovsky, G. Haran, *Proc. Natl. Acad. Sci. USA* **2003**, 100, 3197–3202.
- [16] D. S. Talaga, W. L. Lau, H. Roder, J. Tang, Y. Jia, W. F. DeGrado, R. M. Hochstrasser, *Proc. Natl. Acad. Sci. USA* **2000**, 97, 13021–13026.
- [17] J. M. Harris, S. Zalipsky, *Poly(ethylene glycol): Chemistry and Biological Applications*, American Chemical Society, Washington D.C., **1997**.
- [18] E. Ostuni, R. G. Chapman, R. E. Holmlin, S. Takayama, G. M. Whitesides, *Langmuir* **2001**, 17, 5605–5620.
- [19] S. J. Sofia, V. Premnath, E. W. Merrill, *Macromolecules* **1998**, 31, 5059–5070.
- [20] C. D. Heyes, A. Y. Kobitski, E. Amirgoulova, G. U. Nienhaus, unpublished results.

- [21] S. Jo, K. Park, *Biomaterials* **2000**, 21, 605–616.
- [22] F. M. Veronese, *Biomaterials* **2001**, 22, 405–417.
- [23] T.-W. Cha, V. Boiadjev, J. Lozano, H. Yang, X.-Y. Zhu, *Anal. Biochem.* **2002**, 311, 27–32.
- [24] K. Huang, B. P. Lee, D. R. Ingram, P. B. Messersmith, *Biomacromolecules* **2002**, 3, 397–406.
- [25] B. H. Schneider, E. L. Dickinson, M. D. Vach, J. V. Hoijer, L. V. Howard, *Biosens. Bioelectron.* **2000**, 15, 13–22.
- [26] I. S. Millett, S. Doniach, K. W. Plaxco, *Adv. Protein Chem.* **2002**, 62, 241–261.
- [27] D. O. V. Alonso, K. A. Dill, *Biochemistry* **1991**, 30, 5974–5985.
- [28] H. D. Kim, G. U. Nienhaus, T. Ha, J. W. Orr, J. R. Williamson, S. Chu, *Proc. Natl. Acad. Sci. USA* **2002**, 99, 4284–4289.
- [29] J. N. Forkey, M. E. Quinlan, M. A. Shaw, J. E. T. Corrie, Y. E. Goldman, *Nature* **2003**, 422, 399–404.

Received: January 19, 2004 [200400024]